

THE DESIGN AND CONSTRUCTION OF A SUBCRITICAL
NUCLEAR REACTOR

by

Thomas McKinley Schuler, Jr.

Thesis submitted to the Graduate Faculty of the
Virginia Polytechnic Institute
in candidacy for the degree of

MASTER OF SCIENCE

in

Nuclear Engineering Physics

APPROVED:

APPROVED:

Director of Graduate Studies

Head of Department

Dean of Applied Science and
Business Administration

Supervisor or Major Professor

June, 1957

Blacksburg, Virginia

TABLE OF CONTENTS

	Page
LIST OF FIGURES	4
INTRODUCTION	5
REVIEW OF LITERATURE	7
DESIGN OF THE REACTOR	10
Multiplication Factor	10
Cell Design	13
Basic Dimensions	19
CONSTRUCTION OF THE REACTOR	22
Basic Material	22
Machining Process	22
Stacking	35
Fuel and Source	36
MEASUREMENT OF NEUTRON FLUX IN REACTOR	38
Measurement Technique	38
Method of Application	45
Special Measurements	46
Analysis of Results	47
SUMMARY	62
ACKNOWLEDGMENTS	63
BIBLIOGRAPHY	64

	Page
VITA	66
APPENDIX I	67
APPENDIX II	69

LIST OF FIGURES

Figure		Page
1.	Completed Reactor	12
2.	Variation of ρ , β and the Product $\rho\beta$ with Cell Radius	18
3.	V. P. I. Exponential Reactor Plan View . . .	20
4.	Machining Room	24
5.	Plan View of Solid Blocks	27
6.	Plan View of Reactor Fuels Stringers	30
7.	Plan View of Reactor Foil Stringer	31
8.	Plan View of Reactor Center Blocks	33
9.	Plan View of Reactor Source Block	34
10.	Loaded Fuel Stringer Section	39
11.	Relative Flux Curve (Two Layers Uranium Loaded in Reactor)	50
12.	Relative Flux Curve (Four Layers Uranium Loaded in Reactor)	51
13.	Relative Flux Curve (Six Layers Uranium Loaded in Reactor)	52
14.	Relative Flux Curve (Eight Layers Uranium Loaded in Reactor)	53
15.	Relative Flux Curve (Nine Layers Uranium Loaded in Reactor)	54
16.	Horizontal Traverse Curve	57
17.	Diffusion Length Curve	60
18.	Fermi Age Curve	61

INTRODUCTION

The introduction of a graduate program in Nuclear Engineering Physics at Virginia Polytechnic Institute was made in September, 1956. It became evident that experimental facilities other than the nuclear accelerator and reactor simulator, already installed, would be necessary to give proper instruction in the basic operating principles of reactors and provide additional research equipment.

Considering that a critical reactor would be too expensive to construct and maintain in operation at this early stage of the program, it was proposed that an exponential or subcritical reactor be built. Investigation showed that such a reactor would allow realistic experimentation, while still maintaining a safe and economical mode of operation.

The two basic types of exponential reactors are the light water moderated, natural uranium reactor and the graphite moderated, natural uranium reactor. The light water type required less total material for construction and is smaller in structure, but the presence of the water raises many problems caused by

corrosion. As a consequence, it was decided that the graphite moderated reactor would be preferable.

The reactor was to be constructed of reactor grade graphite and natural uranium, patterned on the exponential assembly at the Oak Ridge School of Reactor Technology. The reactor is to be equipped with a cadmium covered control rod and is to be covered on all surfaces with a cadmium shield at some later date. Besides the measurement of various reactor parameters such as material buckling, diffusion length, Fermi age, and harmonic distortion, studies may be made on the effects of control rods and boundary conditions of reactors. This reactor should prove to be a most versatile laboratory instrument as the nuclear engineering program progresses.

REVIEW OF LITERATURE

The importance of exponential pile experiments was first realized during the period preceding the first chain reaction by Fermi and his collaborators in 1942⁽⁵⁾. At this time, several experiments were made on three uranium graphite systems to determine the respective reproduction or multiplication factors. The exponential reactor has since become an essential part of the vast research program involved in the design of large heterogeneous reactors. Many reactor parameters such as Fermi age, material buckling and diffusion length may be determined by experiment on an exponential reactor at relatively low cost. The exponential reactor has the same lattice structure as the proposed critical reactor but is considerably smaller in size and, therefore, less expensive to build and operate.

The importance of the exponential reactor for research purposes and the theory involved have been carefully put forth by Hughes⁽¹⁶⁾, Murray⁽¹⁹⁾, and Glasstone and Edlund⁽⁸⁾.

In the past few years, many refined experiments have been made to determine various reactor parameters to a high degree of accuracy on the Brookhaven and Argonne exponential piles by Rickey⁽²⁵⁾, and Downe and Kouts⁽³⁾. An extensive program was set up by Dopchie, Leonard, Neve de Meverguier, and Tavernier⁽⁴⁾ to determine the effect of source conditions on the harmonics of the flux in an exponential lattice structure.

The rapid growth of the reactor field since World War II has increased the need for engineers and scientists trained in reactor physics. To this extent the exponential pile has become an important laboratory tool for the instruction of students in basic reactor operational theory. As far as is known, the first exponential pile built principally for pedagogical purposes was installed at Oak Ridge School of Reactor Technology in 1950. Extensive tests were made on this reactor and the results published by Campbell, Wyly, and Howell⁽¹⁾. Since this initial installation, the exponential reactor has been incorporated as a training instrument at the Argonne National Laboratory⁽²⁶⁾ and the Brookhaven National Laboratory.

Many colleges and universities are introducing graduate programs in reactor physics to meet the growing need for qualified reactor specialists. New York University⁽¹⁷⁾ was the first to install a sub-critical reactor for use in the laboratory and it is evident that many other institutions will incorporate this type of reactor into their programs in the future.

DESIGN OF THE REACTOR

Multiplication Factor

The basic difference between a critical and sub-critical reactor is the multiplication factor. The multiplication factor is defined as the ratio of the number of neutrons in one generation to the number of neutrons in the preceding generation. If the multiplication factor is equal to unity, a self-sustaining chain reactor can be maintained and the reactor is considered critical. For a very large reactor or a reactor of infinite dimensions, the multiplication factor is given by⁽⁹⁾

$$k_{\infty} = \epsilon P f \eta \quad (1)$$

where:

- k_{∞} = infinite multiplication factor
- ϵ = fast fission factor
- P = resonance escape probability
- f = thermal utilization
- η = average number of neutrons released per neutron absorbed in uranium.

Thermal utilization is defined as the ratio of the number of thermal neutrons absorbed in fuel to the total number of thermal neutrons absorbed. The resonance escape probability is the fraction of the fast neutrons produced by fission, which escape capture while being slowed down to thermal energies. The fast fission factor is defined as the ratio of the total number of fast neutrons produced by fission due to neutrons of all energies to the number resulting from thermal-neutron fission.

Due to neutron leakage, the multiplication factor for a critical reactor of finite size is given by⁽¹⁰⁾

$$k_{eff} = k_{\infty} \rho \quad (2)$$

where:

- k_{eff} = effective multiplication factor
- ρ = nonleakage probability.

The nonleakage probability is defined as the probability that a neutron will not escape during the slowing down process or while it diffuses as a thermal neutron and is a function of the geometry and material of the particular reactor. Therefore, the design

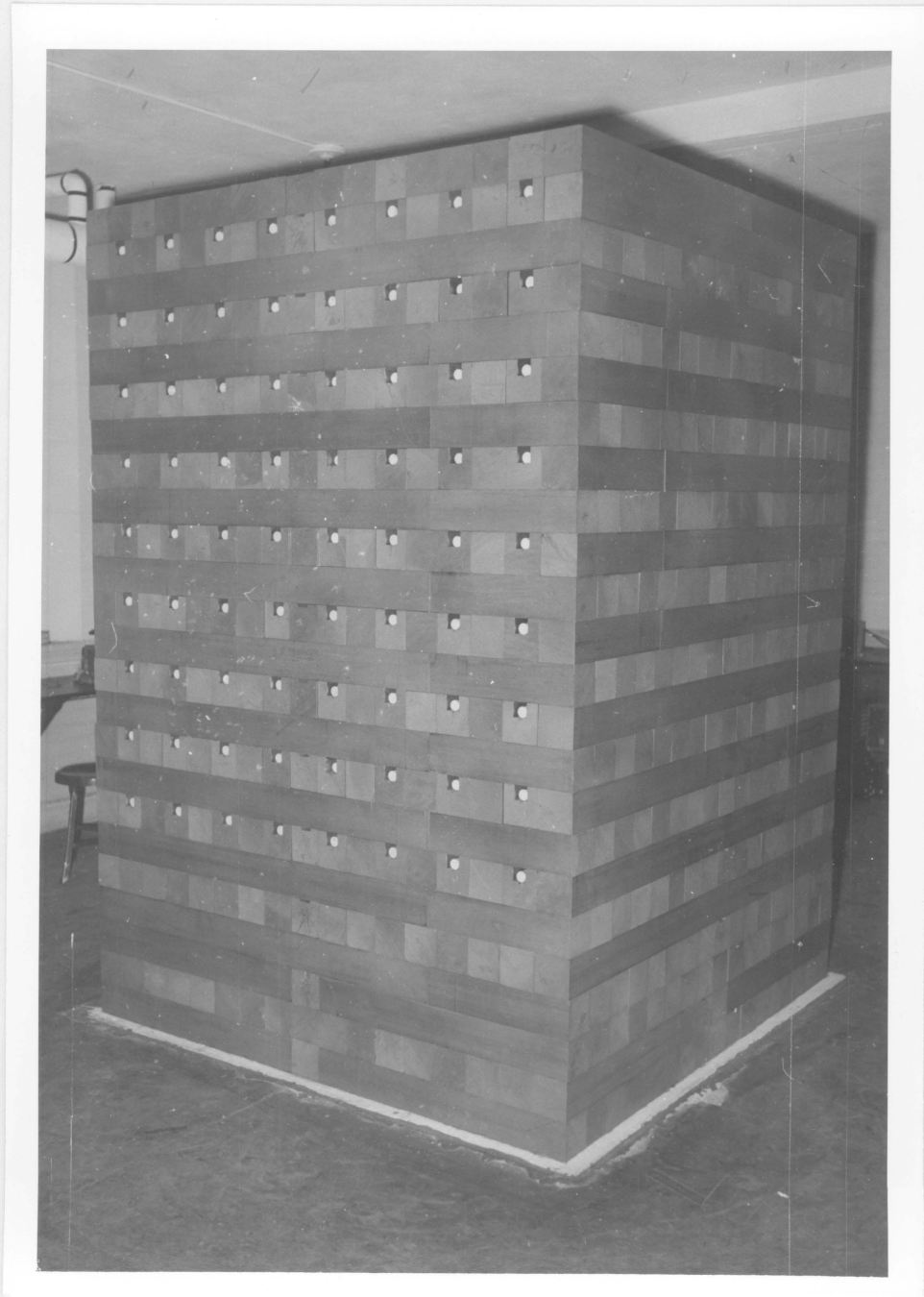


FIG. I COMPLETED REACTOR

should be made so as to make the infinite multiplication factor as large as possible to limit the size of the reactor.

An exponential pile is a subcritical assembly constructed with exactly the same lattice as a critical reactor but appreciably smaller. The exponential pile is approximately one-third the size of the critical reactor and requires an external neutron source to maintain a neutron flux in the lattice. Excessive leakage in the assembly prevents the multiplication factor from approaching unity.

Cell Design

In designing the reactor the basic consideration was the determination of the lattice structure for a critical reactor. On an approximate basis the lattice structure is divided into a number of identical unit cells under the assumption that a square cross-section can be replaced by a circular cross-section of the same area. If the fuel is arranged in parallel elements with each cell consisting of a square cross-section, the equivalent cell of circular cross-section will be a long cylinder.

It was found that natural uranium rods of one inch diameter could be obtained for use as fuel. Therefore, the lattice was designed on the basis of this information.

The average number of neutrons released per neutron absorbed in uranium is 1.32 for natural uranium and the fast fission factor, as taken from published data is 1.03⁽²⁰⁾ for one inch diameter fuel rods. These values remain constant for these particular fuel rods. This leaves the calculation of the resonance escape probability (P) and thermal utilization (f) for some cell radius. Any change in the relative proportions of fuel and moderator which causes f to increase causes P to decrease. Therefore, it is necessary to find the proportion which gives the maximum value for the product Pf . For this reason, calculations were made of P and f for various cell radii and the product plotted, Figure 2, to determine the maximum value and the corresponding cell radius. For fuel rods of one inch diameter this radius will result in the maximum multiplication factor.

The resonance escape probability is given by⁽²¹⁾

$$p = e^{-\frac{V_U \Sigma_U}{V_M \Sigma_M}} \quad (3)$$

where:

V_U = volume of uranium

V_M = volume of moderator

Σ_M = effective macroscopic scattering cross-section for graphite

Σ_U = effective macroscopic scattering cross-section for uranium.

The macroscopic cross-section is determined from

$$\Sigma = \frac{\rho N_0 \sigma}{A} \quad (4)$$

where:

ρ = density of material

N_0 = Avogadro number

A = atomic weight of material

σ = microscopic scattering cross-section of material.

The effective microscopic cross-section for the uranium rods is

$$\sigma_0 = 1.651 \left[1 + \mu \frac{S}{M} \right] \quad (5)$$

where:

$$\begin{aligned} \mu &= 2.67 \text{ for metal slugs} \\ \frac{S}{M} &= \text{ratio of surface area to slug mass.} \end{aligned}$$

Likewise, the effective microscopic scattering for graphite is

$$\sigma_m = \frac{\xi \sigma_s}{5.6} \quad (6)$$

where:

$$\begin{aligned} \sigma_s &= 4.8 \text{ barns between } 0.025\text{ev to } 0.1\text{mev} \\ &\quad \text{for carbon} \\ \xi &= \text{average logarithmic energy decrement} \\ &\quad \text{per collision (0.159).} \end{aligned}$$

The thermal utilization was calculated from the equation (22)

$$\frac{1}{f} = 1 + \frac{V_M \Sigma_M}{V_U \Sigma_U} \cdot \frac{\phi(r_0)}{\phi} + \delta \quad (7)$$

where:

Σ_M and Σ_U = absorption cross-sections

$$\frac{\phi(r_0)}{\phi} = 1 + \frac{(K_0 r_0)^2}{8} - \frac{(K_0 r_0)^4}{192} \quad (8)$$

where:

r_0 = fuel rod radius

$K_0 = 0.70 \text{ cm}^{-1}$ for uranium.

The excess absorption term δ is given by

$$\delta \simeq \frac{(K_1 r_1)^2}{2} \left(\ln \frac{r_1}{r_0} - \frac{3}{4} \right) \quad (9)$$

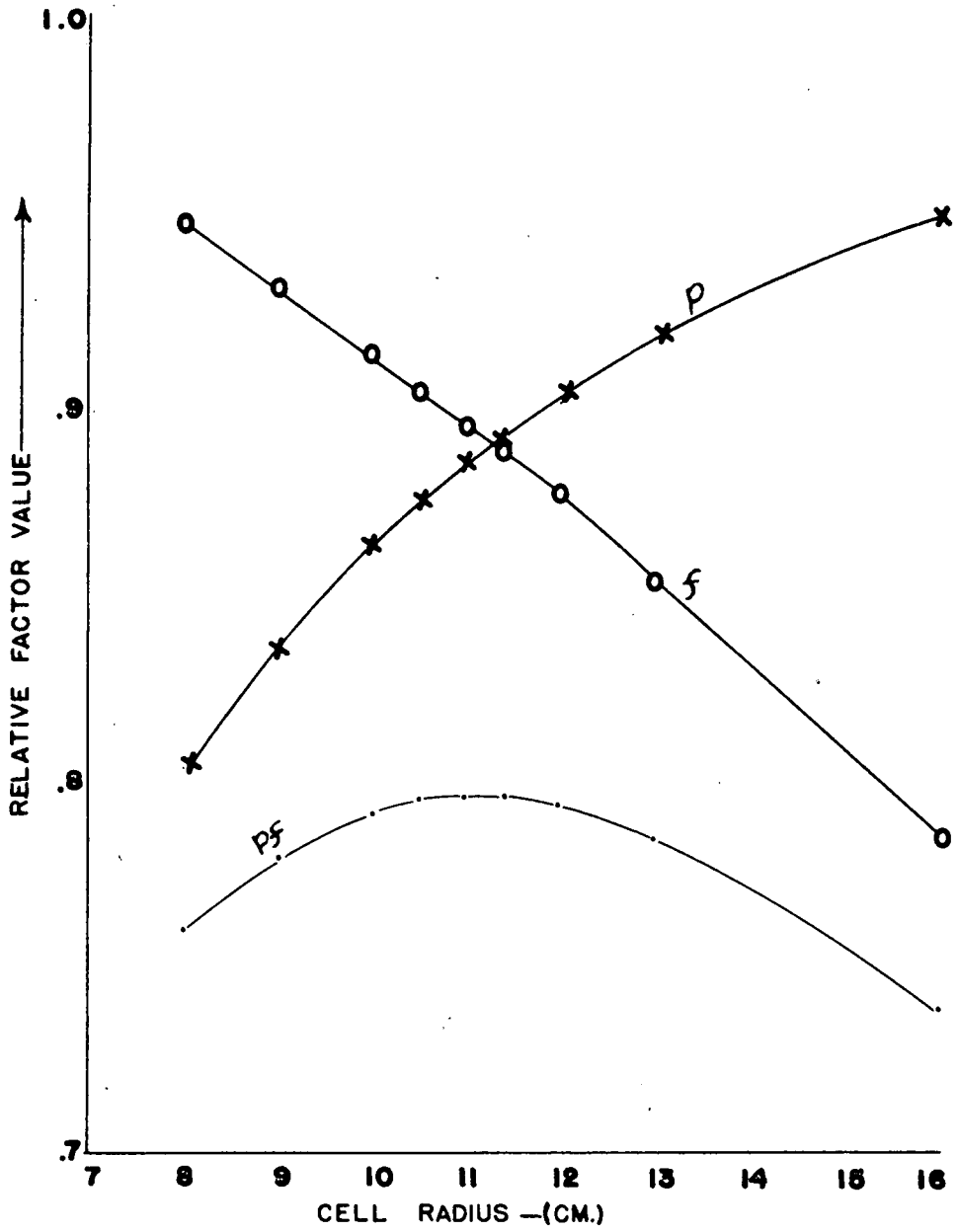
where:

r_1 = radius of cell

$K_1 = 0.02 \text{ cm}^{-1}$ for graphite.

A complete sample calculation of P and f may be found in Appendix I.

FIG.2 VARIATION OF P , f AND THE PRODUCT Pf WITH CELL RADIUS



Examination of Figure 2 shows that the maximum value of P_f will occur if the radius of the unit circular cell is 11.45 centimeters. Converting this circular area to a square of equal area in square inches results in a distance of eight inches between fuel rods. Therefore, the lattice was constructed so as to place the fuel rods eight inches apart.

Basic Dimensions

To facilitate this spacing it was decided to construct the reactor from lengths of graphite of four inch cross-section. The over-all dimensions of the reactor were determined primarily by the size of the room designated as the reactor laboratory.

It was desired to have the lattice structure, Figure 3, constructed as a cube. In addition, a graphite pedestal was needed so that the source could be placed at least a diffusion length below the bottom of the lattice thereby permitting the majority of the source neutrons to be thermalized by the time they reached the lattice structure.

The ceiling of the laboratory limited the total height of the structure to ten feet. It was then

HOLE TO BASE OF SLUG LATTICE

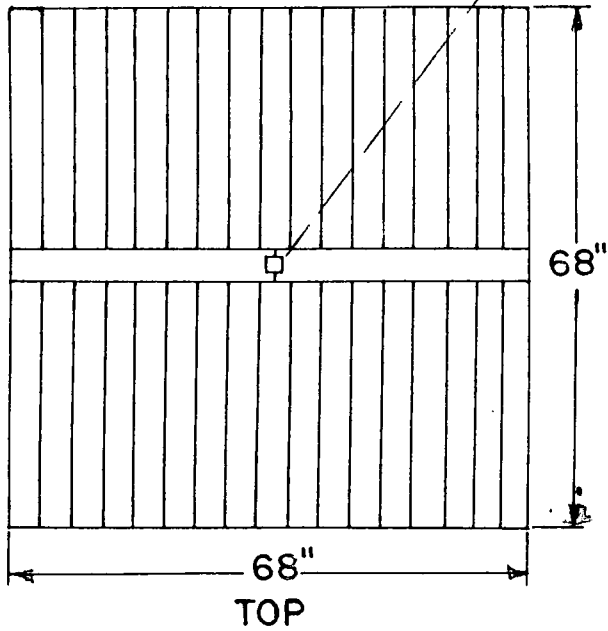
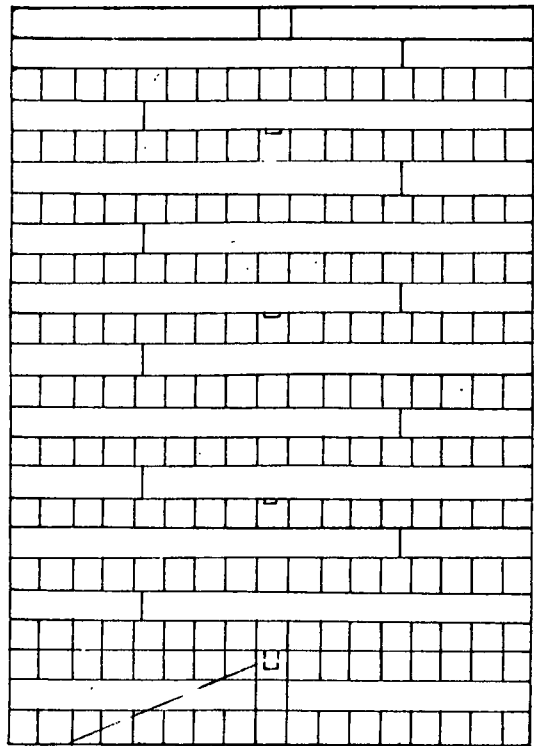
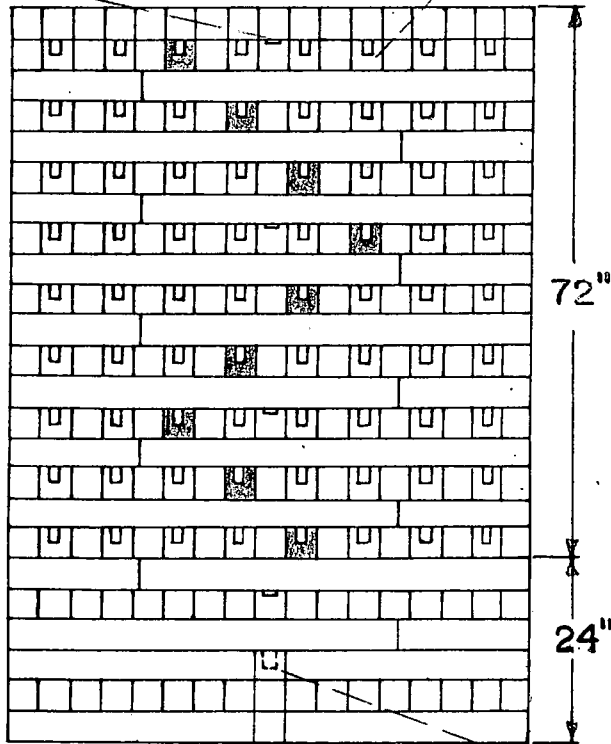


FIG. 3
V. P. I.
EXPONENTIAL REACTOR
PLAN VIEW
SCALE = 1/25


UNDERCUT FUEL
STRINGER

FOIL STRINGER FUEL STRINGER



decided that the pedestal would be two feet in height with the cube having a side dimension of six feet, thereby allowing a two foot clearance at the top of the reactor for insertion of a control rod into the center of the reactor. Since the central stringers of a 72 inch cube would contain fuel, the width and length of the pile were reduced to 68 inches. This reduction placed a solid stringer at the center of the reactor on each layer with a fuel rod on either side. These solid stringers were cut to form the control rod hole, Figure 3.

The resulting structure had over-all dimensions of 68 x 68 x 96 inches with a lattice structure placing the fuel rods eight inches apart. This lattice spacing resulted in nine rows of eight fuel stringers each for a total of 72 fuel stringers as shown in Figure 3.

CONSTRUCTION OF THE REACTOR

Basic Material

The reactor was constructed of AGOT reactor grade graphite obtained from the National Carbon Company. The graphite was made from petroleum coke with an apparent density of 1.7 grams per cubic centimeter and a boron content of 0.5 parts per million. The graphite was received from the manufacturer in bars of 4.37 x 4.37 inch cross-section and 51 inch length. In the production of the blocks the graphite was extruded⁽²⁾ to form the square cross-section and cut off to the 51 inch lengths. Five hundred and forty-four blocks were used in the construction of the reactor.

Due to the oversize dimensions of the blocks and the roughness of the surfaces, it was necessary to machine the graphite down to the proper sizes as designed.

Machining Process

The actual construction procedure began on June 11, 1956. The first phases of the operation consisted of setting up the machinery necessary to process the

graphite in some locality where the resulting graphite dust would cause no damage to the housing structure and there would be sufficient ventilation for the workers. A condemned building on the campus was selected for this purpose.

Based on the work of Fermi and his collaborators on the original graphite pile⁽⁶⁾, ordinary wood working machines were used. A thickness planer, a jointer, and a large table saw were installed in such a manner as to form a production line, Figure 4. In addition to cross ventilation from the windows and doors of the machining room, an exhaust fan and associated piping were installed on the planer to pull the dust from the planer into a smaller room where the dust was bagged for resale at some later date. An industrial type vacuum cleaner was also used on the jointer to remove the graphite dust.

The machining process started by passing the blocks through the planer four times, once on each side, to remove the scale formed by the extruding process and to increase the accuracy of the finishing cuts made on the blocks. It was found that the accuracy of both the jointer and planer was decreased

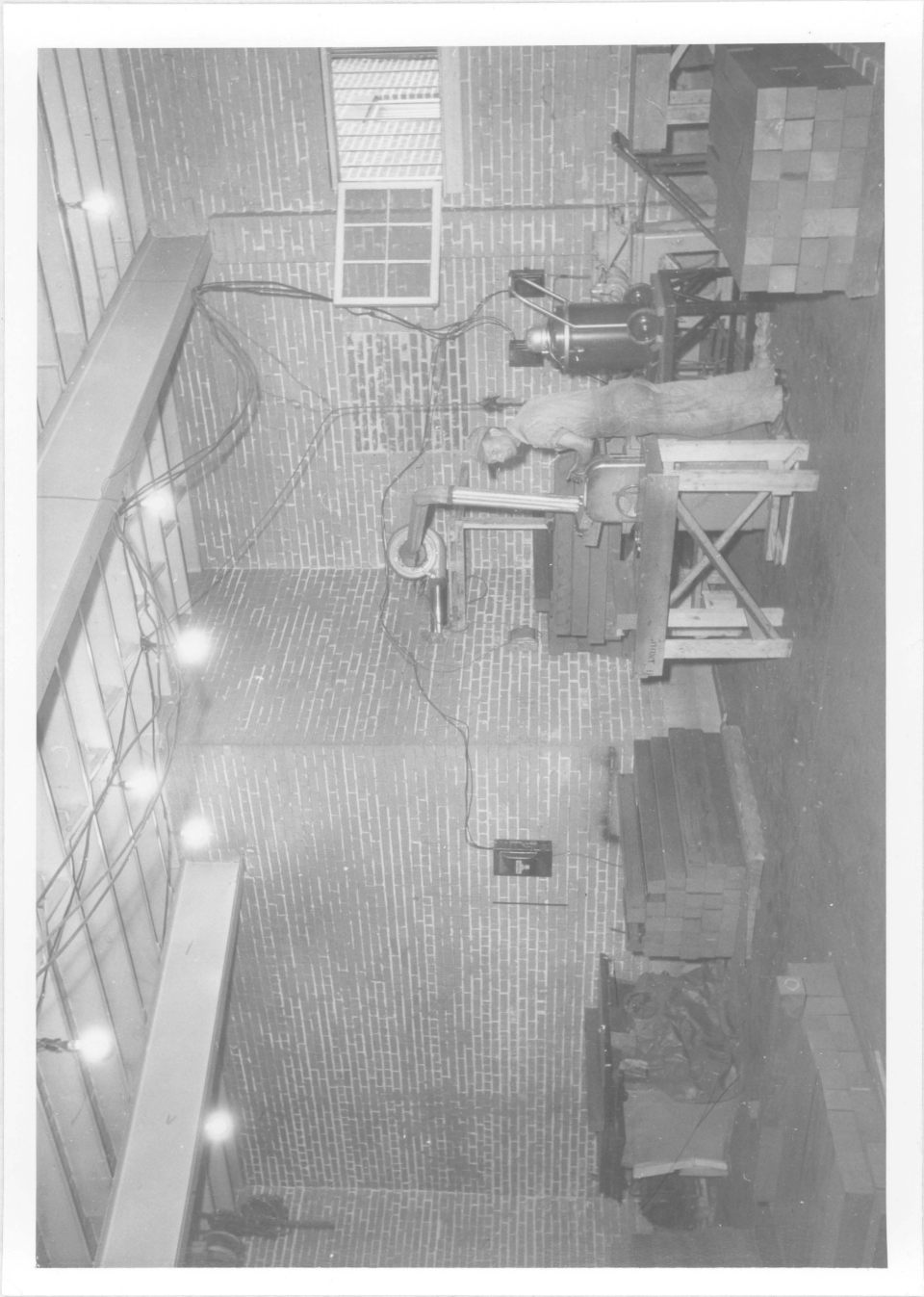


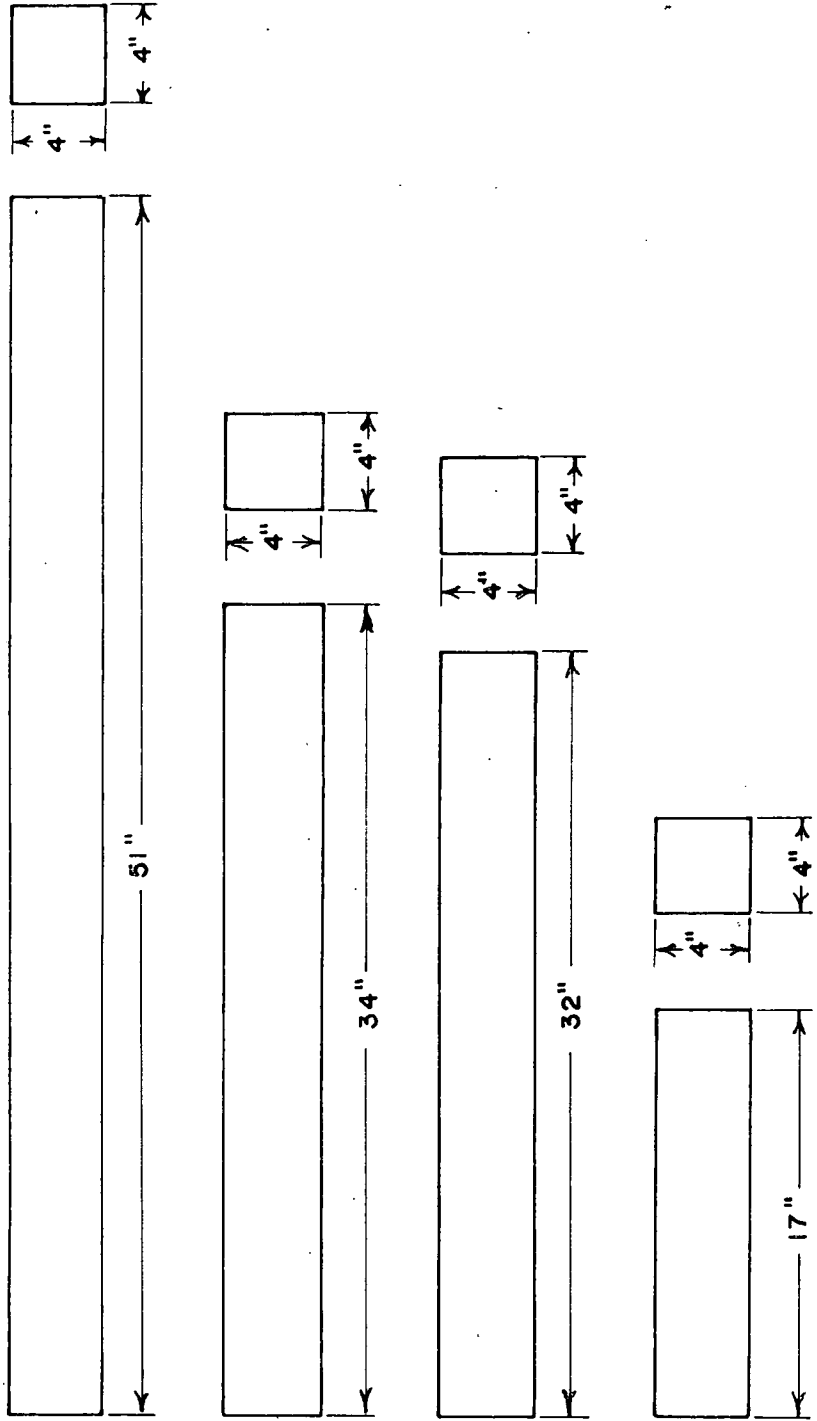
FIG. 4 MACHINING ROOM

as the depth of cut made by each machine increased. Therefore, the first cuts made on the planer were made as deep as possible to increase the accuracy of the later cuts made on the jointer and planer. Two surfaces were made plane and perpendicular to each other on the jointer. This required a jointer cut on two adjacent sides. The blocks were then passed through the planer two more times for the final finish cuts. Each cut was made on the side opposite and parallel to the jointer cut, thereby producing a square cross-section. The dimensions of the finished block were held to a tolerance of ± 0.005 inch. All bars had a basic cross-section dimension of four inches. The blocks were then passed on to the table saw to be cut to the proper lengths with a tolerance of ± 0.625 inch.

Several difficulties were encountered during this part of the procedure as a result of the physical condition of the graphite blocks as received from the manufacturer. As mentioned previously, the blocks were covered with a hardened scale. This scale dulled the blades of the machines in a very short time. High speed steel blades were used on the jointer and the

planer. It became necessary to resharpen the blades after each eight hour period of machining or after approximately 60 blocks had been machined. The main difficulty resulted from the bows and twists in the unfinished blocks. The machinery would not remove a bow or twist from a block which had a deformity in an excess of one-eighth inch at the maximum point. To solve this problem it was decided to cut these bowed and twisted blocks into 17 inch lengths, thereby eliminating the deformities or decreasing the error to a point at which the machinery could remove the remaining irregularities. Needless to say this procedure greatly increased the labor and time necessary to finish the process. Another problem was found in the final act of cutting the blocks to the required lengths. Figure 5 shows the finished blocks in correct lengths of 17 to 51 inches. It was found that some of the blocks were less than 51 inches in length. These particular blocks had to be cut to some smaller length while still utilizing as much of the graphite as possible. Consequently, the blocks were cut into lengths of 17 and 32 inches. By placing two 32 inch blocks so that they butt up against the

FIG. 5 PLAN VIEW OF SOLID BLOCKS
SCALE $\frac{3}{16}'' = 1''$



sides of a block of four inch cross-section, the required 68 inch length could be made. Examination of Figure 3 shows four complete layers constructed in this manner.

A total of 186 blocks were cut to a length of 34 inches. Sixty of these blocks plus one 51 inch block were undercut by 1/100 inch to insure sliding in the reactor.

As many of the remaining blocks as possible were cut to a length of 51 inches. The 17 inch blocks resulting from the cutting of the 32 inch and 34 inch lengths were used with the 51 inch lengths to form the 68 inch width of the reactor.

The finished blocks of graphite were then transferred by truck to Davidson Hall for the final machining process and stacking. Care was taken during the transfer to brush each block with dry scrub brushes to remove any loose graphite dust or impurities from the outer surfaces. Due to the high neutron capture cross-section of sodium, precautions were taken throughout the machining of the graphite to keep the surfaces free of perspiration and all foreign materials.

The machining of the fuel, foil, and control rod slots was done on a large milling machine. A clamp type jig was made and installed on the mill bed to hold the graphite blocks during the cutting process.

Fuel slots were cut in 144 of the 3/4 inch blocks as shown in Figure 6. The slots were cut by two regular 1/2 inch wide milling cutters with a 1/2 inch steel fly cutter between the standard cutters to form the wedge cut in the bottom of the slot. The wedge cut was introduced to insure the proper centering of the fuel rods. Eighteen of the fuel blocks were of the undercut type and were placed in the reactor so that large objects could be irradiated at various positions in the reactor. Figure 3 shows these undercut stringers as shaded blocks.

The foil slots were cut by three 1/2 inch wide milling cutters held together to make a 1-1/2 inch cut 3/8 inch deep in 14 undercut, 3/4 inch blocks as shown in Figure 7. Undercut blocks were used to facilitate removal of the foil stringers. In addition to the foil slots a 2-1/2 x 1-1/4 inch cut was made in one end of each foil stringer and in one end of each of the remaining 28 undercut, 3/4 inch blocks

FIG. 6 PLAN VIEW OF REACTOR FUEL STRINGER
TOTAL NUMBER IN REACTOR = 144
SCALE $\frac{3}{8}'' = 1''$

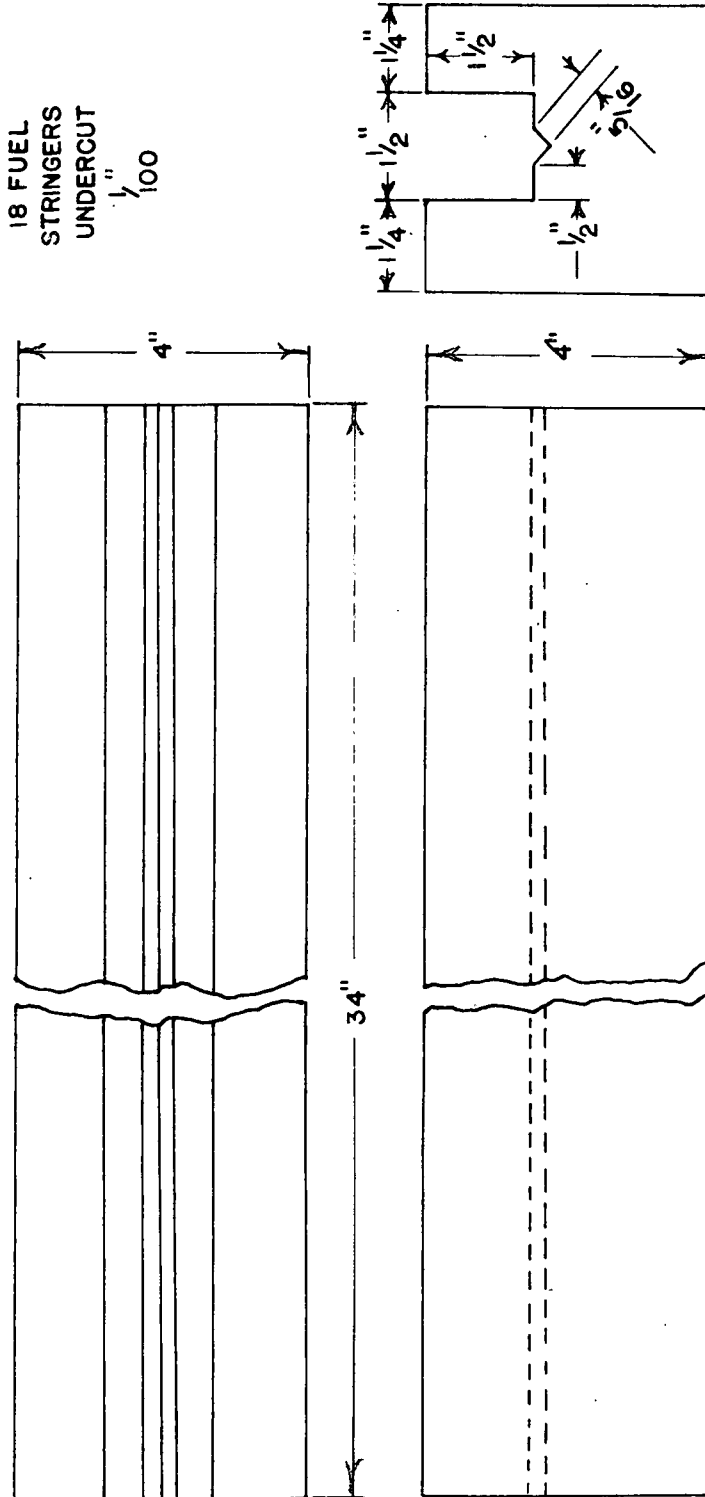
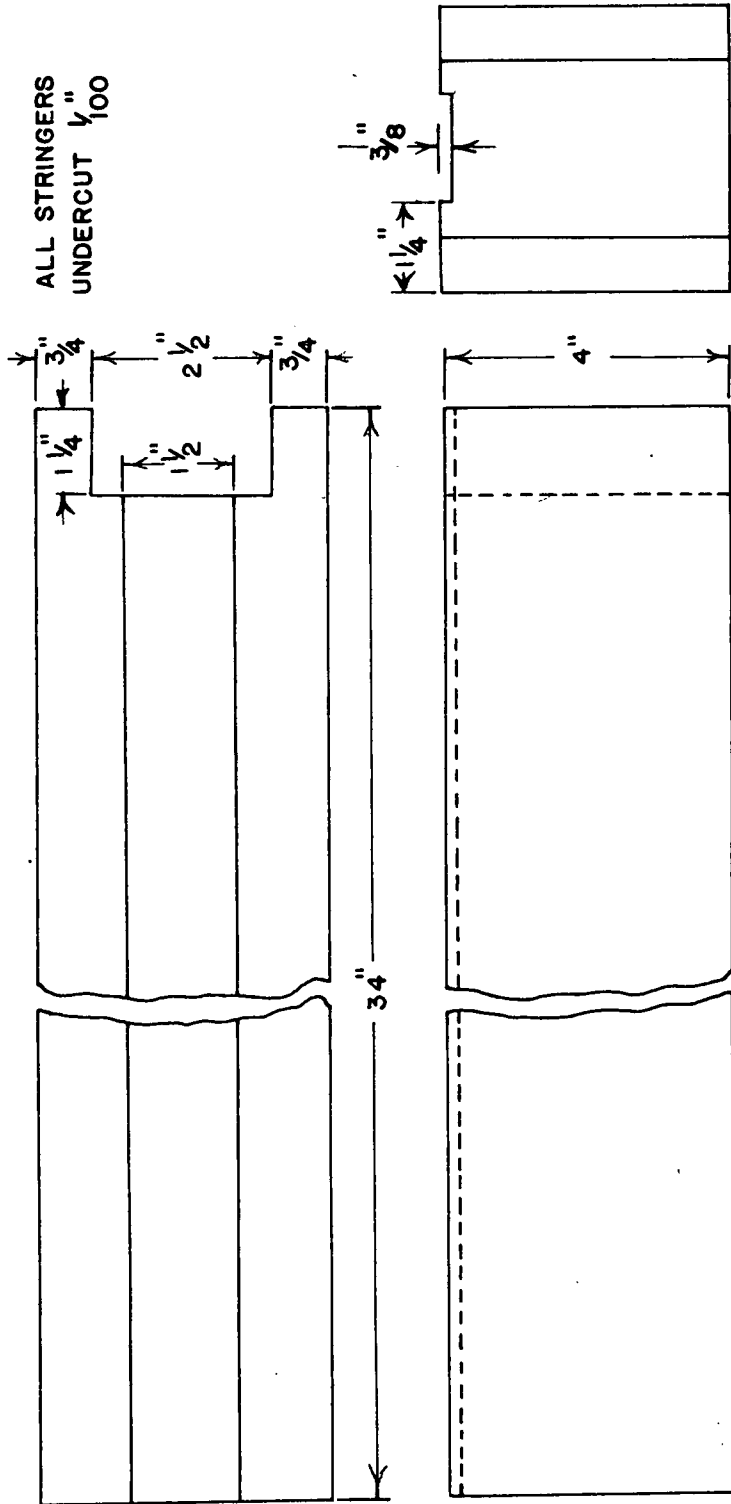


FIG. 7 PLAN VIEW OF REACTOR FOIL STRINGER
TOTAL NUMBER IN REACTOR = 14
SCALE $\frac{3}{8}'' = 1''$



as shown in Figures 7 and 8. These blocks were used as the center stringer of each layer above the source stringer, thereby forming a 2-1/2 x 2-1/2 inch hole from the top of the reactor to the base of the slug lattice. This was done to provide a place for the introduction of a control rod into the reactor. All of these blocks may be removed and turned around so that the solid ends fill the control rod hole if necessary in performing special types of experiments.

A small, free hand cut, machined on a small milling machine, was made in the foil slot, perpendicular to the slot, of each foil stringer near the end of the block. This was done so that a small hook could be used to pull the stringer out of the reactor. No definite dimensions were used for this cut.

The source stringer was the final block to be machined. A standard 1-1/2 inch diameter drill was used to drill the 2-1/4 inch deep hole in the one undercut, 51 inch block, as shown in Figure 9. The source hole was cut 34 inches from one end of the stringer so as to place the source at the exact center of the reactor. Again, a free hand L-shaped cut was made on the end of the block so that a hook could be

FIG 8 PLAN VIEW OF REACTOR CENTER BLOCKS
TOTAL NUMBER IN REACTOR = 28
SCALE $\frac{3}{8}$ "

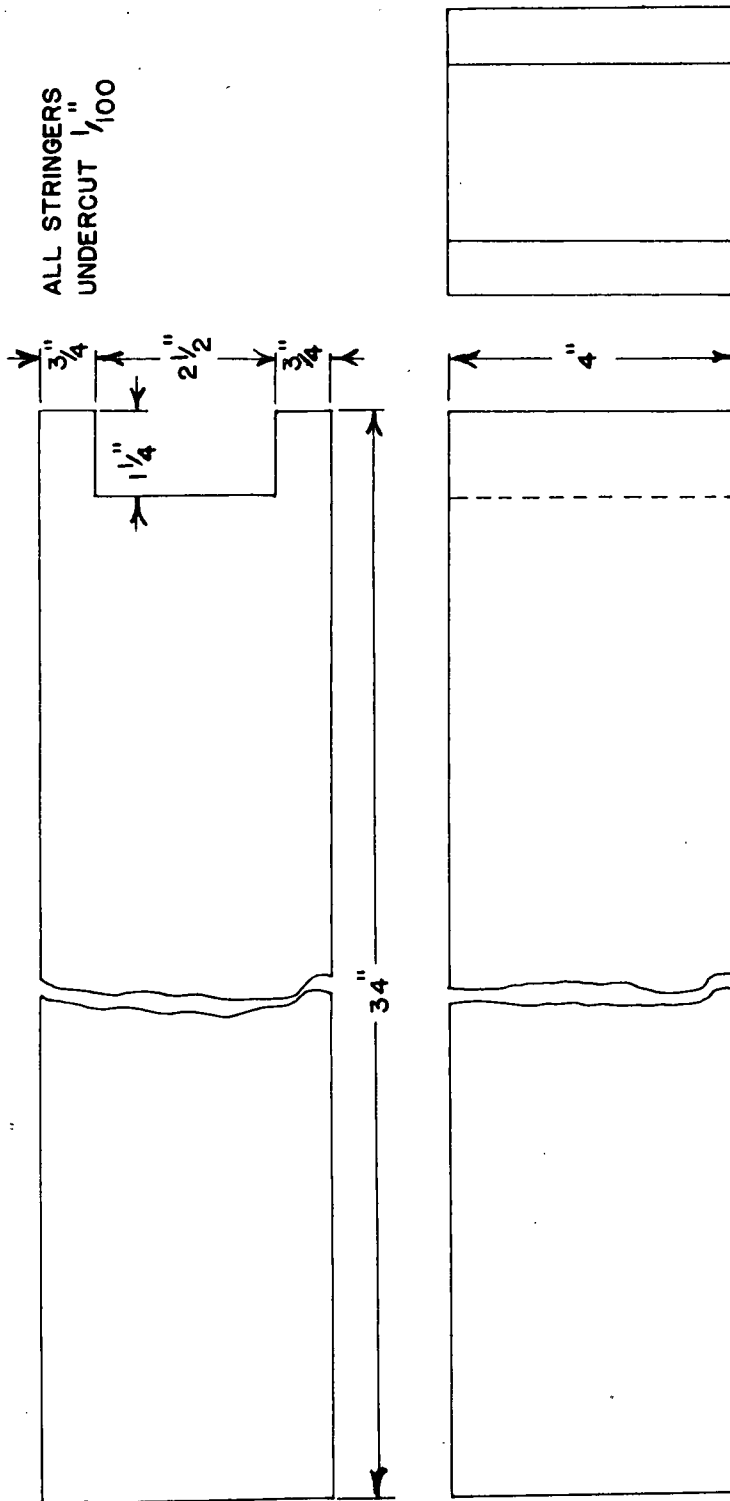
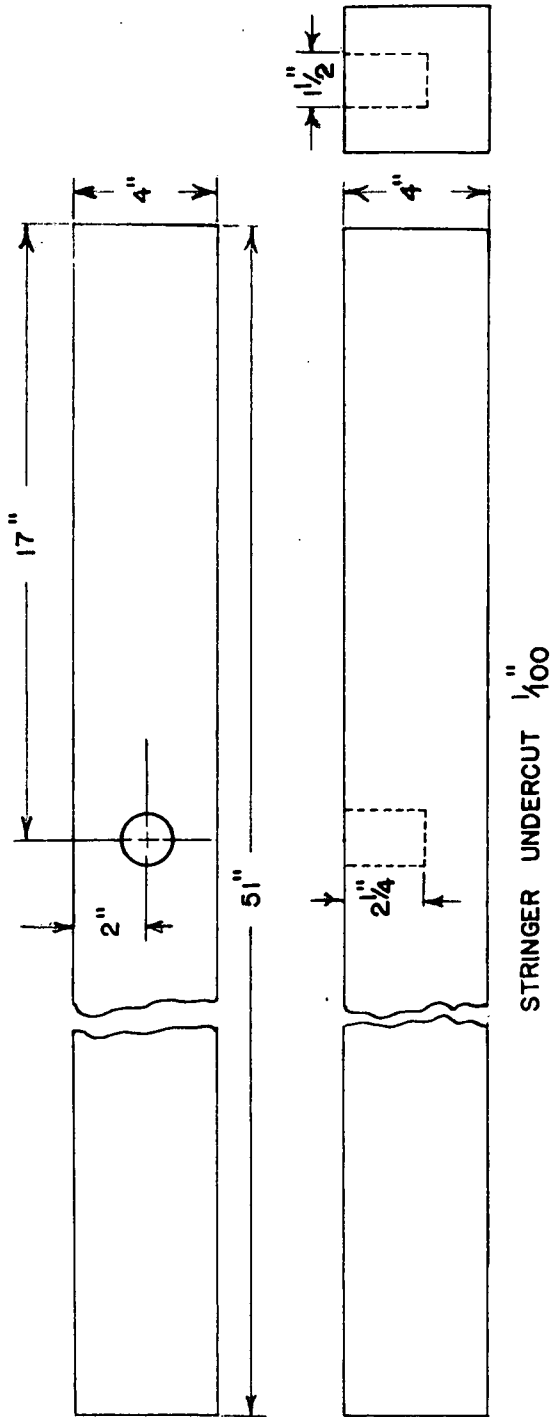


FIG. 9 PLAN VIEW OF REACTOR SOURCE BLOCK

SCALE $\frac{3}{16}'' = 1''$



used to pull the stringer for removal or insertion of the source.

Stacking

The graphite blocks were stacked on a reinforced concrete pad built into the floor of the reactor laboratory room. The pad extended through the floor and two feet into the ground to provide a firm foundation for the reactor, which weighs approximately 16 tons when fully loaded.

The stacking procedure consisted first of the construction of a 24 inch pedestal, including the source stringer and second, the construction of the fuel lattice as shown in Figure 3. Three complete layers of the pedestal were made of 32 inch blocks with a 17 inch and 51 inch block forming the center stringer. As each block was put into place it was again thoroughly brushed with dry scrub brushes to remove all dust and impurities present on the surfaces. The first stacking of the pile was completed on October 15, 1956.

Fuel and Source

To complete the reactor the natural uranium fuel and source had to be placed in the graphite pile.

The full fuel load consists of 576 natural uranium rods canned in aluminum which measure eight inches in length and one inch in diameter. The uranium was obtained on loan from the United States Atomic Energy Commission at Oak Ridge, Tennessee. Actually, 590 rods were received from the Commission, thereby leaving an extra 14 rods not used in the reactor. Each of the 72 fuel slots holds eight of these fuel rods when fully loaded. The initial loading of the reactor was accomplished by placing uranium rods in only two layers at a time. This allowed proper testing to be carried on during the loading procedure. This process will be discussed further in the neutron flux measurement section.

A 15 curie polonium-beryllium source was also obtained on loan from the AEC through the Mound Laboratory at Miamisburg, Ohio. The steel contained source had, upon arrival, a neutron emission of 3.82×10^7 neutrons per second at a neutron efficiency of 87.3

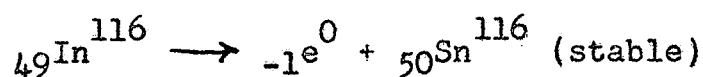
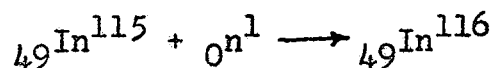
per cent. The source was shipped in a paraffin filled 55 gallon oil drum. The drum is now being used as a storage container for the source when it is not in use in the reactor.

MEASUREMENT OF NEUTRON FLUX IN REACTOR

Neutron flux measurements were made as the reactor was loaded, Figure 10, with the uranium slugs to check the proper operation of the pile and also to determine the effect of various amounts of uranium on the neutron flux along the vertical axis of the reactor. The uranium slugs were loaded two layers at a time. Flux measurements were made with two, four, six, eight, and nine layers of fuel loaded, resulting in five complete tests. All tests were carried on with the source in the reactor.

Measurement Technique

Foil activation was the method utilized for the detection of the neutron flux. Indium foils were used for the detection process since the neutron cross-section at the resonance peak is 28,000 barns at 1.44ev., with the nuclear reactions being⁽²³⁾



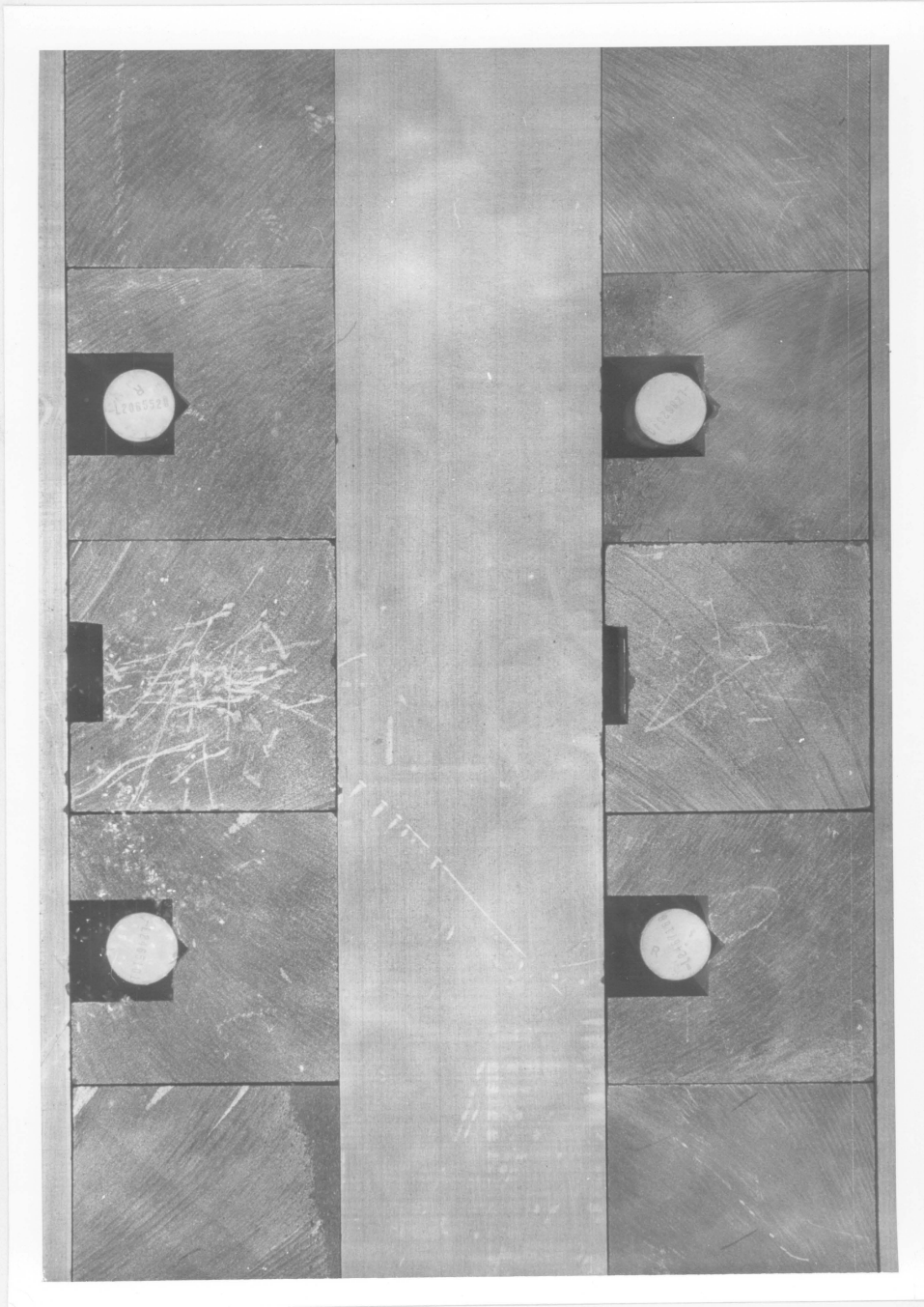


FIG.10 LOADED FUEL STRINGER SECTION

The foils were irradiated for 24 hours before each measurement. The irradiated foils were then counted by a standard end-window counter and the counts recorded on a commercial counting unit consisting of linear amplifier and scaler. The diameter of the counter was 1-3/8 inch with the foil 3/4 inch away. The foils were properly centered under the window with the plane of each foil parallel to the plane of the window. The entire counting assembly was surrounded by lead bricks.

The neutron flux is related to the activity of the foils by the following equation⁽¹¹⁾

$$\phi = \frac{A_{\infty}}{\Sigma_A V} \quad (10)$$

where:

A_{∞} = saturated activity, where exposure periods are large compared to the half life of the foil material

V = volume of foil

Σ_A = neutron cross-section of indium.

The activity at some period of time after removal of the foils from the reactor is⁽¹¹⁾

$$A = A_{\infty} [1 - e^{-\lambda t_e}] [e^{-\lambda t}] \quad (11)$$

where:

A = activity at some time (t) after removal of foil from reactor

λ = radioactive decay constant of ${}^{116}\text{In}$

t_e = exposure time.

Since the counter performs an integration of the activity over the count period, the counts may be given as

$$N = G \int_{t_d}^{t_d+t_c} A dt \quad (12)$$

where:

A = activity at some time, t

G = geometric constant

t_d = delay time between removal of foil and start of count period

t_c = count time.

Substituting equation (2) into equation (3) and integrating gives

$$N = \frac{GA_{\infty}}{\lambda} [1 - e^{-\lambda t_e}] [e^{-\lambda t_d}] [1 - e^{-\lambda t_c}] \quad (13)$$

The actual total count registered will include a background count also; therefore,

$$N_t = \frac{GA_{\infty}}{\lambda} [1 - e^{-\lambda t_e}] [e^{-\lambda t_d}] [1 - e^{-\lambda t_c}] + (B.R.) t_c \quad (14)$$

where:

N_t = total count registered

$B.R.$ = background count rate in counts per unit time.

Solving for A_{∞} and substituting the result into equation (1) gives

$$\phi = \frac{\lambda [N_t - (B.R.) t_c]}{GV \Sigma_a [1 - e^{-\lambda t_e}] [e^{-\lambda t_d}] [1 - e^{-\lambda t_c}]} \quad (15)$$

Since all the foils activated were made of the same material and were of the same size, V and Σ_a are constant for relative measurements and may be disregarded. In addition, the exposure times and delay times were also held constant. Therefore, for a given geometry, the relative flux equation reduces to

$$\phi = \frac{N\epsilon - (B.R.)\tau_c}{1 - e^{-\lambda\tau_c}} \quad (16)$$

The count period was varied with the relative activity of the foils to insure good count statistics. Long background counts were made to obtain a good background rate value. This value was obtained by dividing the total background count by the count time.

Since the time periods involved in the actual count and the background count differed, the error in actual β counts is a function of two errors. The fractional error in actual count is given by

$$\frac{1}{\sqrt{N\epsilon}} \quad (17)$$

Therefore, the error in counts equals

$$\frac{1}{\sqrt{N_c}} \cdot \frac{N_c}{1 - e^{-\lambda t_c}} \quad (18)$$

The fractional error in background counts is

$$\frac{1}{\sqrt{A}} \quad (19)$$

where:

A = total number of background counts taken.

This gives a background error of

$$\frac{1}{\sqrt{A}} \cdot \frac{(B.R.)T_c}{1 - e^{-\lambda t_c}} \quad (20)$$

The total error is then 0.6745 times the square root of the sum of the squares of each error, which results in the following equation:

$$\text{Total Error} = \pm \frac{0.6745}{1 - e^{-\lambda t_c}} \sqrt{N_c + \frac{(B.R.)^2 T_c^2}{A}} \quad (21)$$

Combining equations (7) and (12) gives the relative flux at a point as

$$\phi = \frac{Nt - (B.R.)T_c}{1 - e^{-\lambda T_c}} + \frac{.6745}{1 - e^{-\lambda T_c}} \sqrt{\frac{Nt + (B.R.)^2 T_c^2}{A}} \quad (22)$$

The half life of ${}_{49}\text{In}^{116}$ is 54.1 minutes. The radioactive decay constant is related to the half life by the equation

$$\lambda = \frac{\ln 2}{\text{HALF LIFE}} \quad (23)$$

Therefore, the decay constant for ${}_{49}\text{In}^{116}$ is given as

$$\lambda = .0128/\text{MIN.} \quad (24)$$

Method of Application

The five loading measurements were made with the foil stringers arranged so that four stringers ran perpendicular to one reactor face through the central vertical axis. The remaining three stringers ran

perpendicular to the adjacent face of the reactor. Figure 3 shows this arrangement. The foils, measuring one inch in diameter and 0.005 inch thick, were placed in the foil stringers on aluminum trays and positioned $5\text{-}\frac{3}{4}$ inches from the central vertical axis. The first foil was ten inches above the source with a foil every 12 inches up the reactor axis to a height of 82 inches.

A sample analysis of the flux determination, which was of the same form for all measurements, is given in Appendix I.

Special Measurements

To show the versatility of the reactor for training purposes, additional tests were made to determine the diffusion length, the Fermi age and the degree of harmonic distortion as determined by a horizontal traverse.

The diffusion length measurement was made in a manner similar to the loading measurements except that only the source was present in the reactor and the foils were placed at eight inch intervals starting

with the first foil 18 inches above the source. Nine foils were used for this experiment.

For the Fermi age measurement the foil stringers were arranged perpendicular to adjacent reactor faces as before, at four inch intervals along the vertical axis. Seven foils were used with the first foil ten inches above the source. The central stringers of each layer were reversed so as to fill in the control rod hole. The foils were positioned 2-3/4 inches from the central vertical axis of the reactor.

The horizontal traverse was made with the indium foils placed at 5-3/4 inch intervals across the full width of the reactor on a line passing through the center axis of the reactor. This measurement was made at the 32 inch level of the reactor utilizing a total of eight foils.

Analysis of Results

The thermal neutron flux, in a reactor of this type, has a distribution along any line parallel to the central vertical axis and not close to the

vertical boundaries which is given by the solution of the general equation⁽¹²⁾

$$\nabla^2 \phi + B_m^2 \phi = 0 \quad (25)$$

where:

ϕ = thermal flux

B_m^2 = material buckling constant.

The simplest solution of equation (16) is

$$\phi = \sum_{m=1}^{\infty} \sum_{n=1}^{\infty} A_{mn} \cos \frac{m\pi x}{a} \cos \frac{n\pi y}{b} \sinh \gamma_{mn} (c-z) \quad (26)$$

where:

A_{mn} = arbitrary constant

m, n = integers

a = length of lattice cell

b = width of lattice cell

c = height of lattice cell

z = height above bottom face of cell

$$\gamma_{mn} = \sqrt{\left(\frac{m\pi}{a}\right)^2 + \left(\frac{n\pi}{b}\right)^2 - B_m^2}$$

For points along the Z axis 100 centimeters or more from the source this solution reduces to

$$\phi = ce^{-\gamma z} [1 - e^{-2\gamma(c-z)}] \quad (27)$$

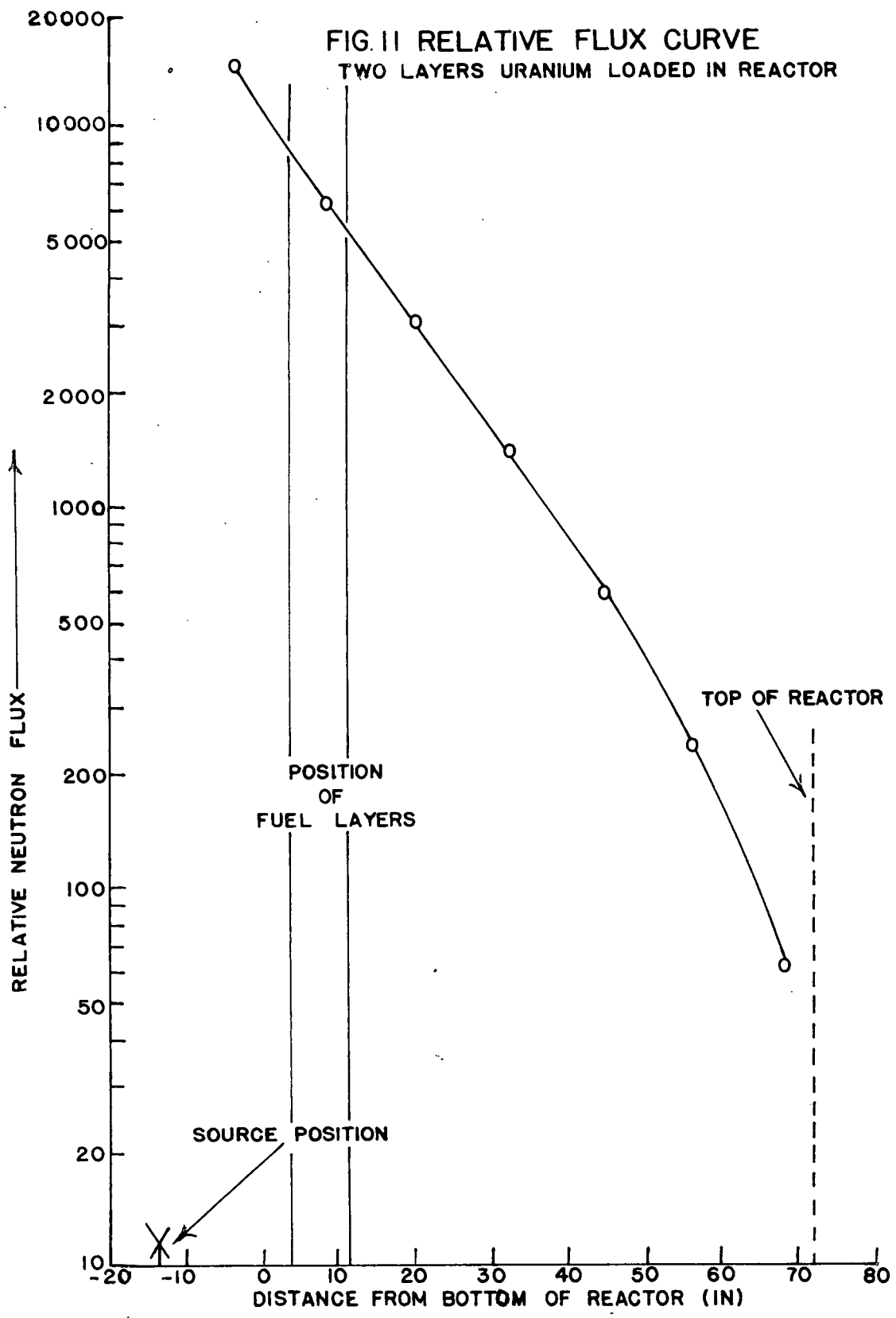
Provided the distances Z do not approach c the equation takes the form

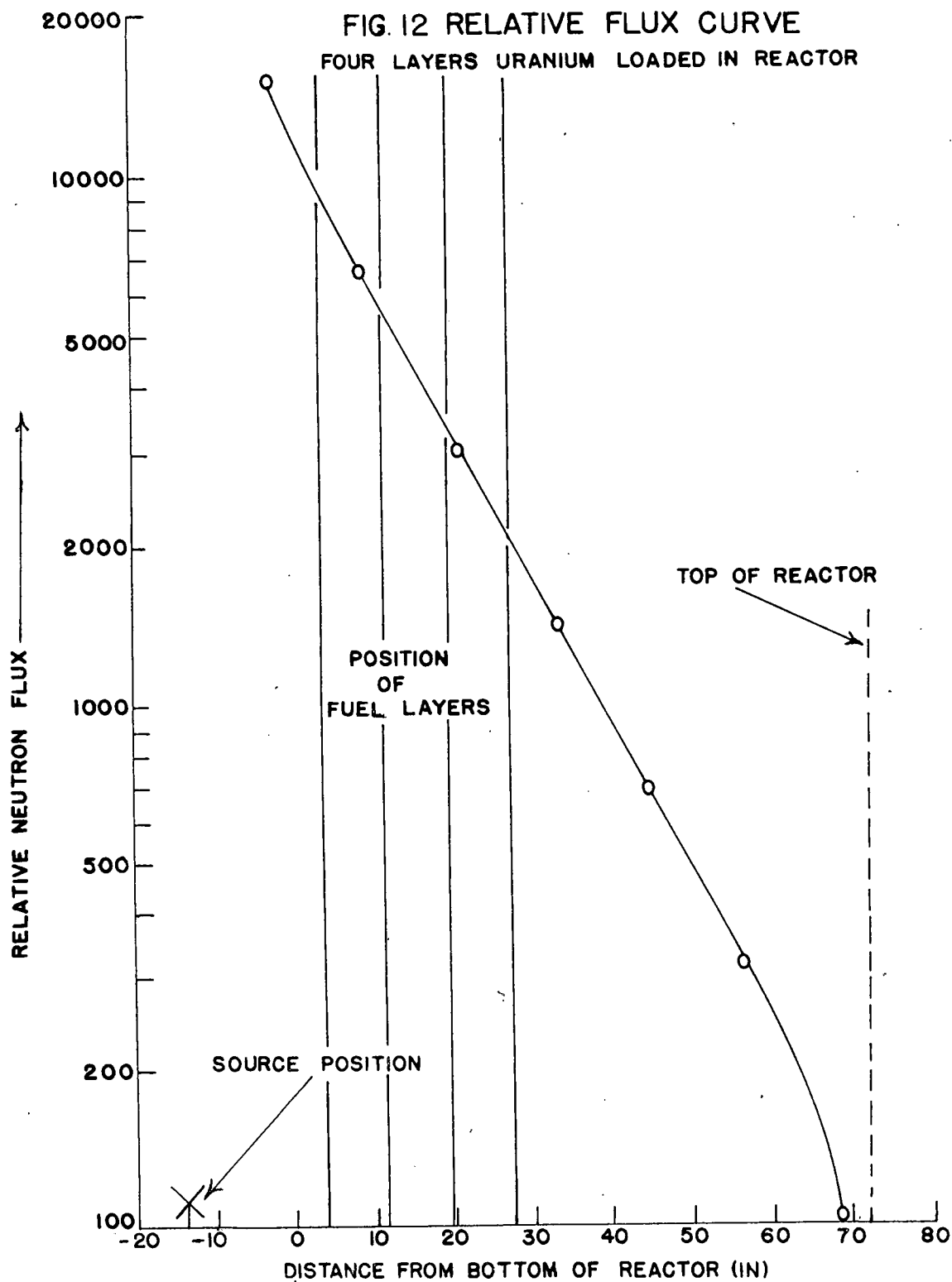
$$\phi = ce^{-\gamma z} \quad (28)$$

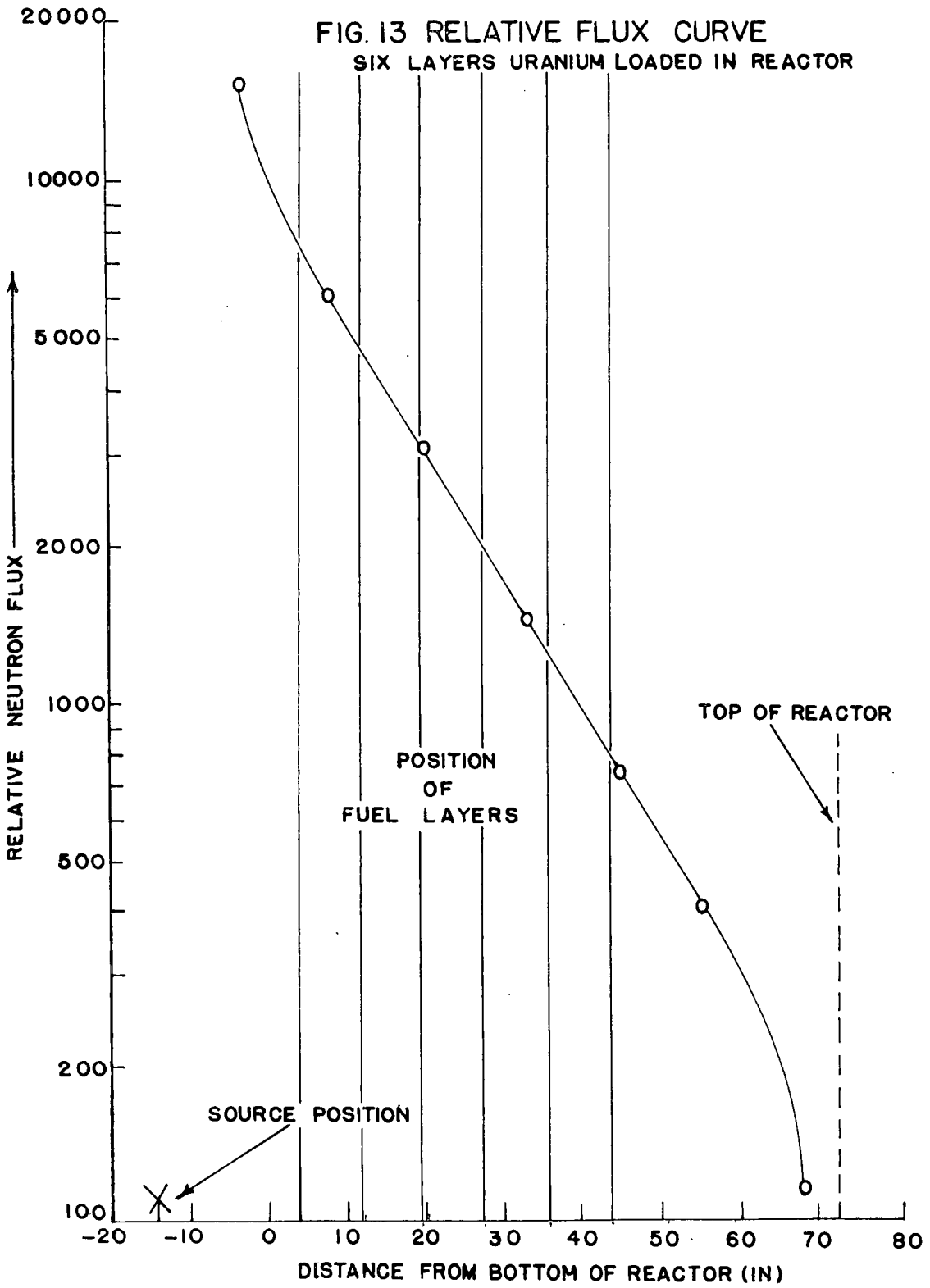
Since the flux falls off in an exponential manner this type reactor is referred to as an "exponential reactor" and the semi-log plot of the flux should be a straight line for the points not too near the boundaries.

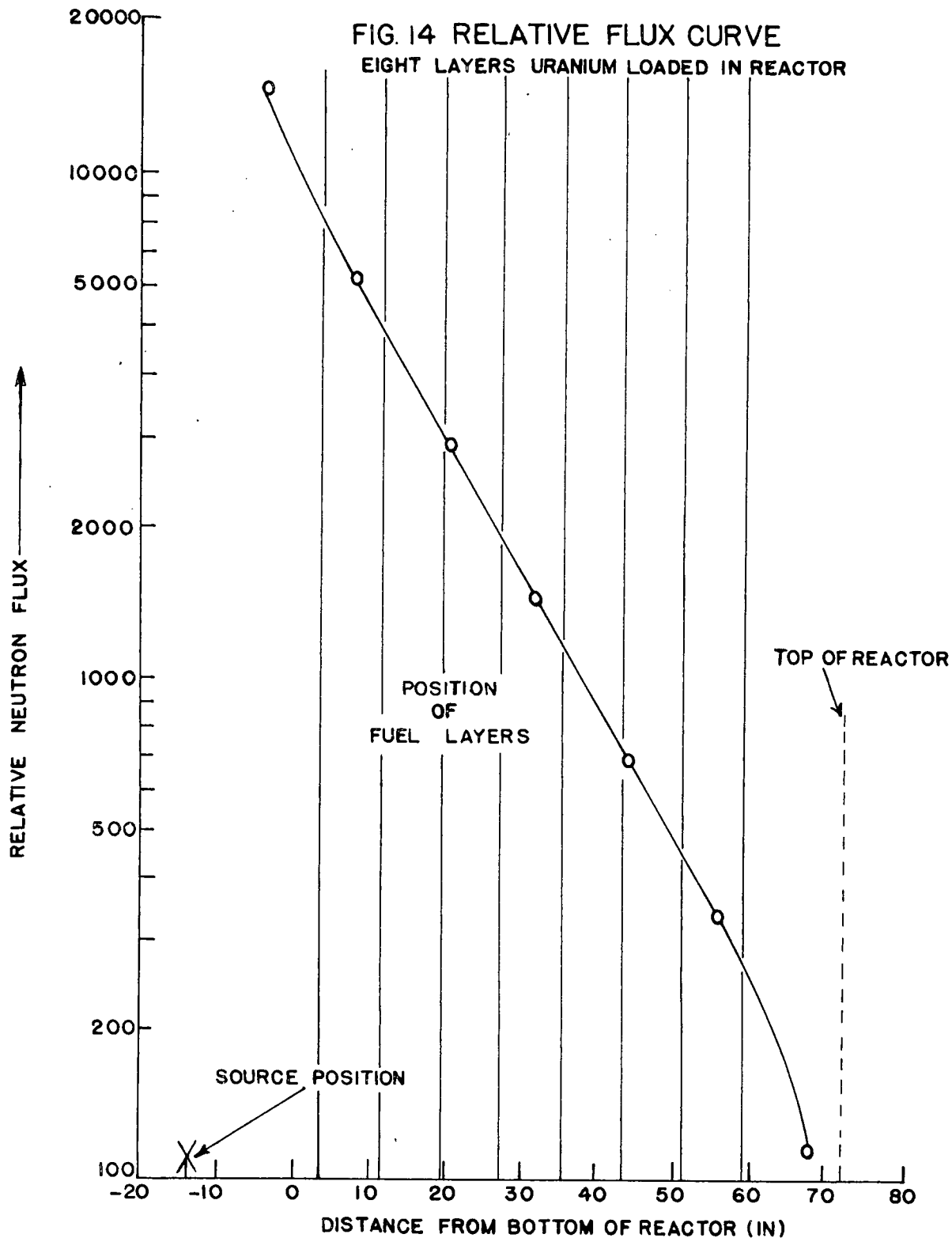
The resulting relative flux values for the five loading measurements were plotted on semi-log coordinate, Figures 11, 12, 13, 14, and 15, as a function of the vertical distances from the foils to the bottom of the lattice cell.

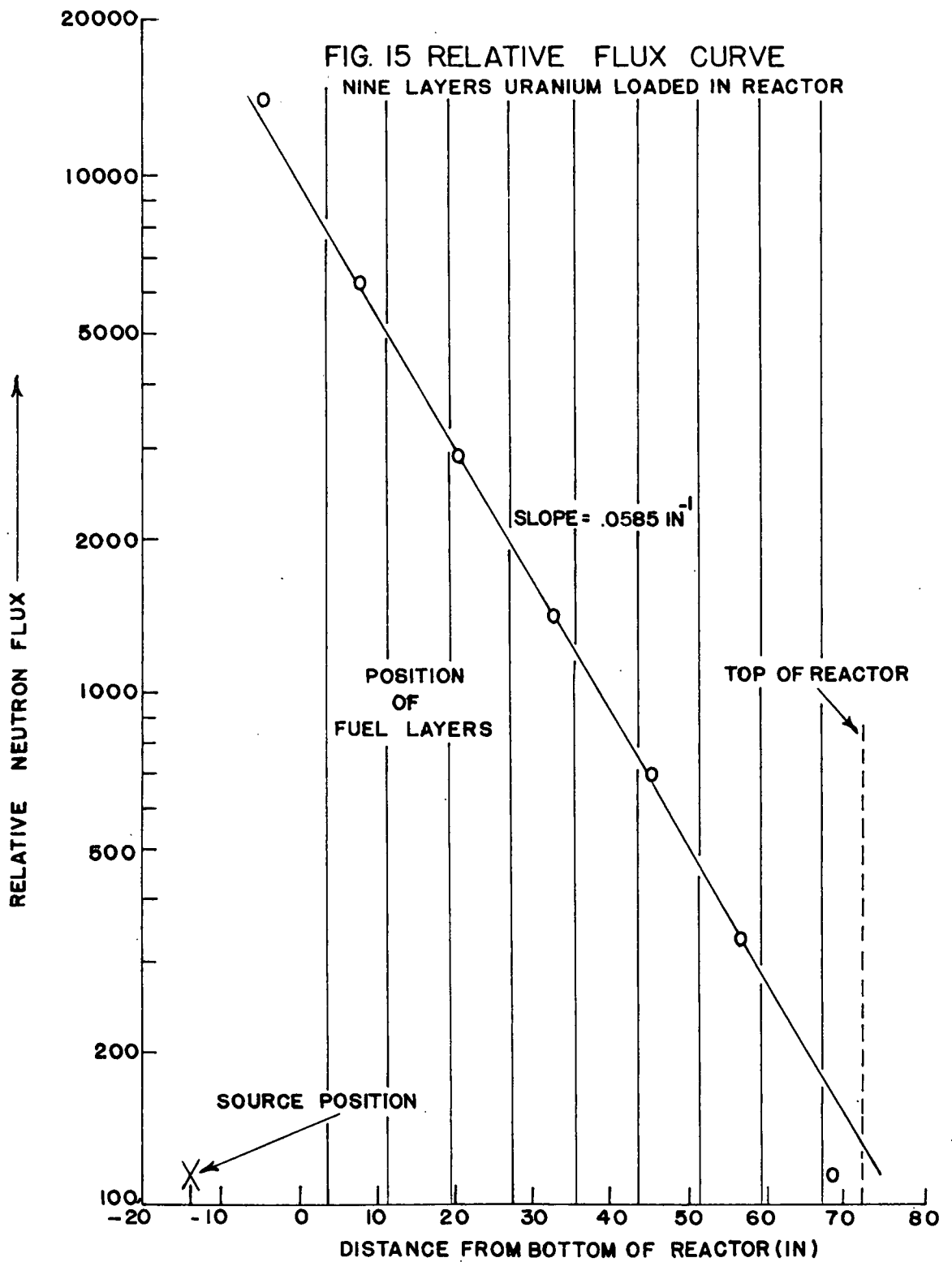
The first point on each curve is of little experimental value since at this distance above the source the neutrons are not completely thermalized. Likewise,











the last point is of little value since it represents the flux near the top of the lattice cell where considerable leakage occurs. Figures 11, 12, 13, 14, and 15 show the tendency of the flux to hold to a fairly constant slope and relative value at points below the level of the last fuel layer loaded in each respective case. The flux above the last layer in each measurement falls off to lower values, although it should be noticed that this flux has actually increased in value when compared to the flux measurement of the preceding test. Comparison of the relative flux curves, Figures 11 and 15, for the two layer measurement and the nine layer measurement shows a maximum increase of approximately 101 per cent in the relative neutron flux at the upper points on the curve.

The neutron flux of the fully loaded reactor, Figure 15, as a function of the distance along the vertical axis is a straight line, disregarding the end points. The material buckling of the reactor for the given lattice materials and structure may be

determined from the slope of this curve by the equation⁽¹³⁾

$$B_m^2 = \left[\frac{\pi}{a} \right]^2 + \left[\frac{\pi}{b} \right]^2 - \gamma^2 \quad (29)$$

where:

γ = slope of curve of flux in fully loaded reactor

provided the harmonic distortion is negligible. In order that the harmonic distortion be disregarded, the curve, Figure 16, of the horizontal traverse should be a cosine curve. Examination of Figure 16 will show that the horizontal traverse curve is within 2 per cent of a cosine curve and, therefore, the harmonic correction may be neglected.

This results in a material buckling for this particular lattice structure of $0.0006/\text{in.}^2$. The critical dimensions for a cube are given by⁽¹⁴⁾

$$a = \frac{\sqrt{3}\pi}{B_g} \quad (30)$$

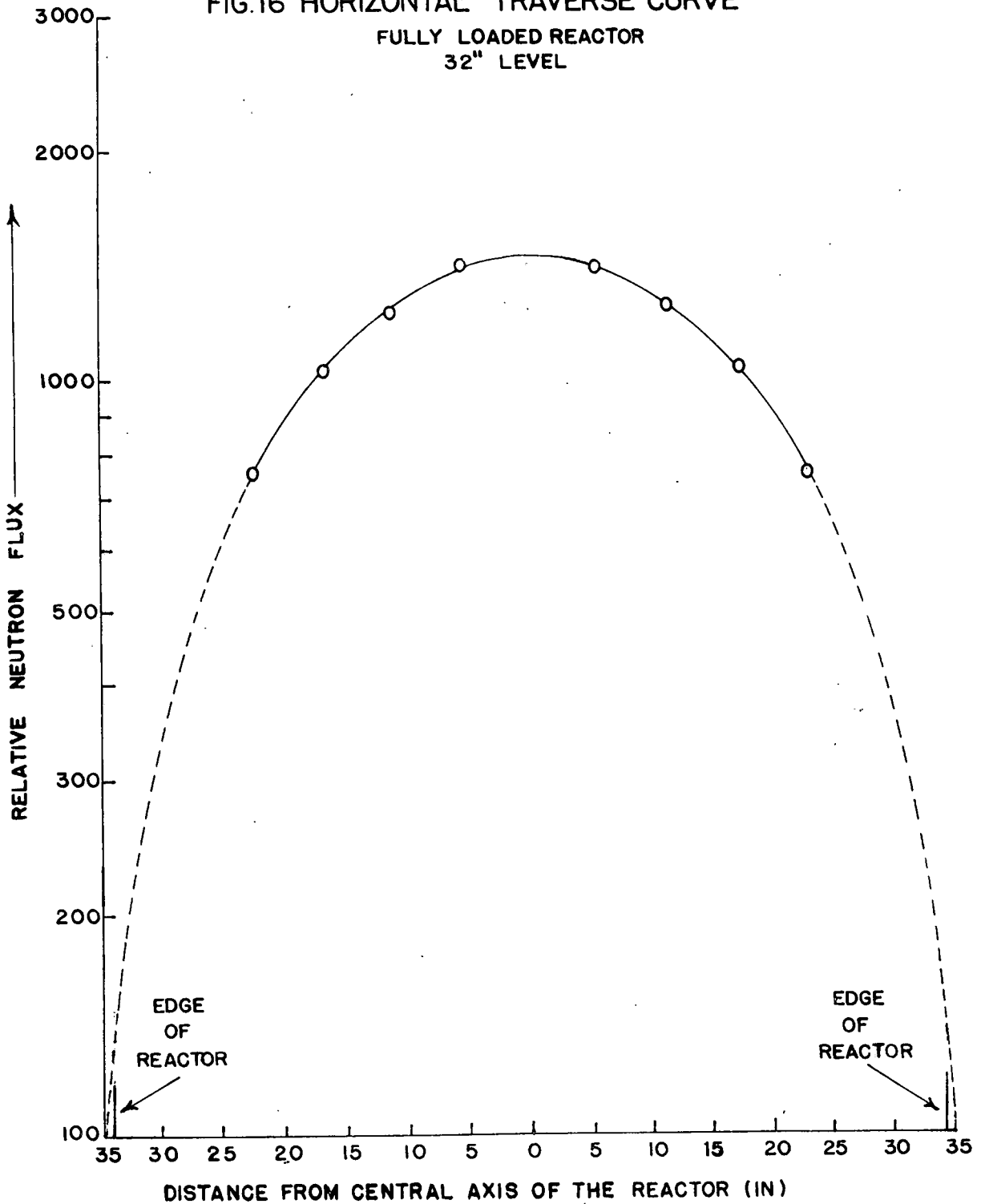
where:

a = side of critical cube including the extrapolated boundaries

B_g = B_m in critical calculation.

FIG.16 HORIZONTAL TRAVERSE CURVE

FULLY LOADED REACTOR
32" LEVEL



This material buckling value results in a critical cube measuring 18.5 feet on a side. This value is in good agreement with published data on a critical reactor of the same lattice structure and material which measures 18 feet on a side.

The resulting relative flux values of the diffusion length experiment were plotted in a manner similar to the loading experiments and resulted in a straight line curve with a slope of 0.0766/in. The last two points on the curve were neglected because these points represent positions near the upper boundary of the reactor.

The diffusion length squared is one-sixth of the mean square distance that a thermal neutron travels from the point at which it is thermalized to the point where it is captured. For a parallelepiped of moderator material the diffusion length is given by⁽²³⁾

$$\frac{1}{L^2} = \gamma^2 - \left[\frac{\pi}{a} \right]^2 - \left[\frac{\pi}{b} \right]^2 \quad (31)$$

where:

- L = diffusion length
- a = length of parallelepiped
- b = width of parallelepiped
- γ = slope of flux curve

provided the flux is not measured at points too near the boundaries of the parallelepiped.

The resulting slope of the diffusion length curve, Figure 17, when applied to equation (22) and corrected for graphite density gave a diffusion length of 57.5 centimeters. This value is also in good agreement with published values of 50 centimeters⁽²⁴⁾.

The Fermi age is defined as one-sixth of the mean square distance traveled by a neutron from the time of its emission to the time at which its age is τ . In the case of thermal reactor this is an important quantity since the square root of the age is the slowing down length of the thermal neutron. The relative neutron flux, Figure 18, was plotted against the square of the distance from the source and resulted in a straight line with a slope of 0.00452 in.^{-2} . The Fermi age is related to the slope of this curve by the equation⁽¹⁵⁾

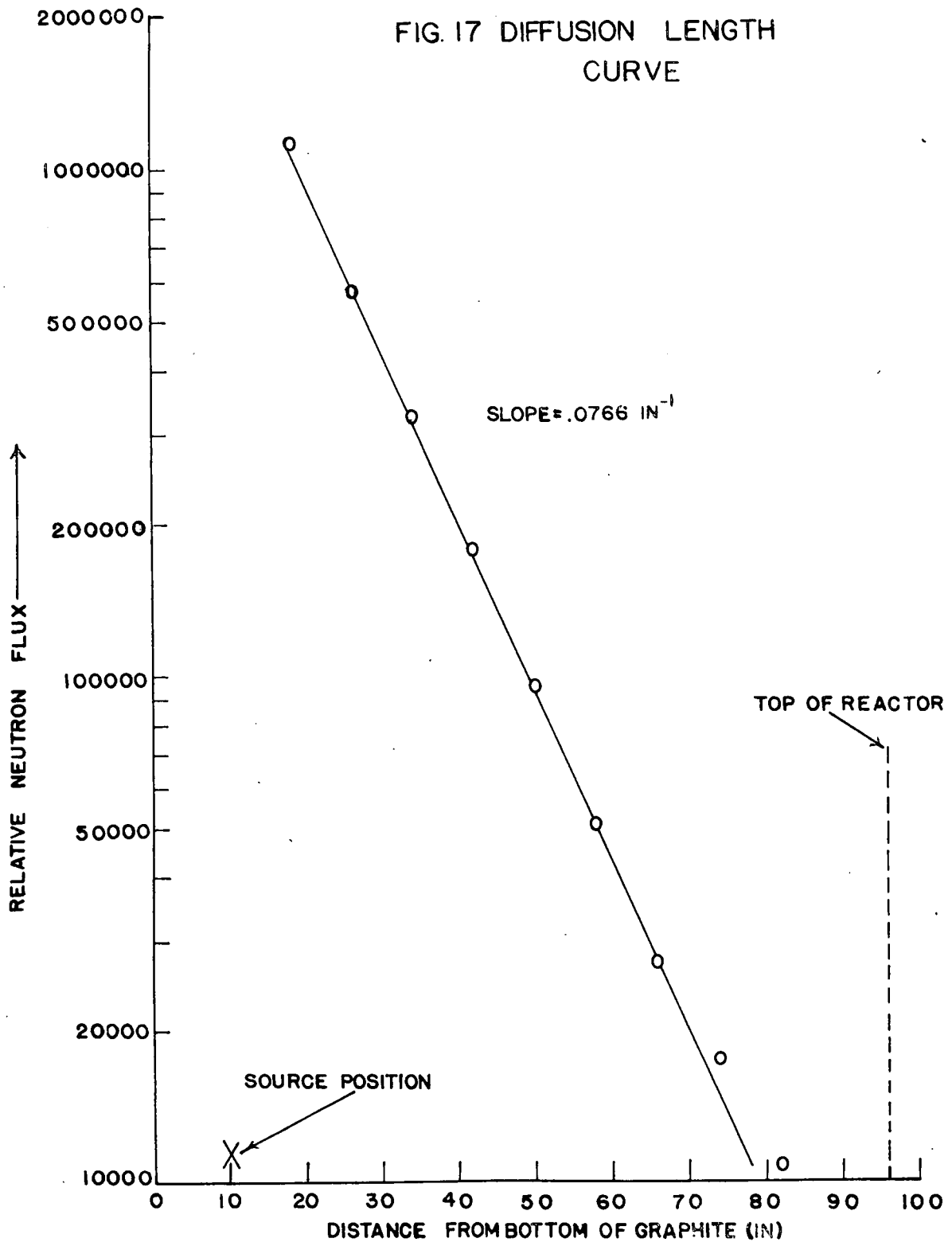
$$\text{slope} = \frac{1}{4\tau} \quad (32)$$

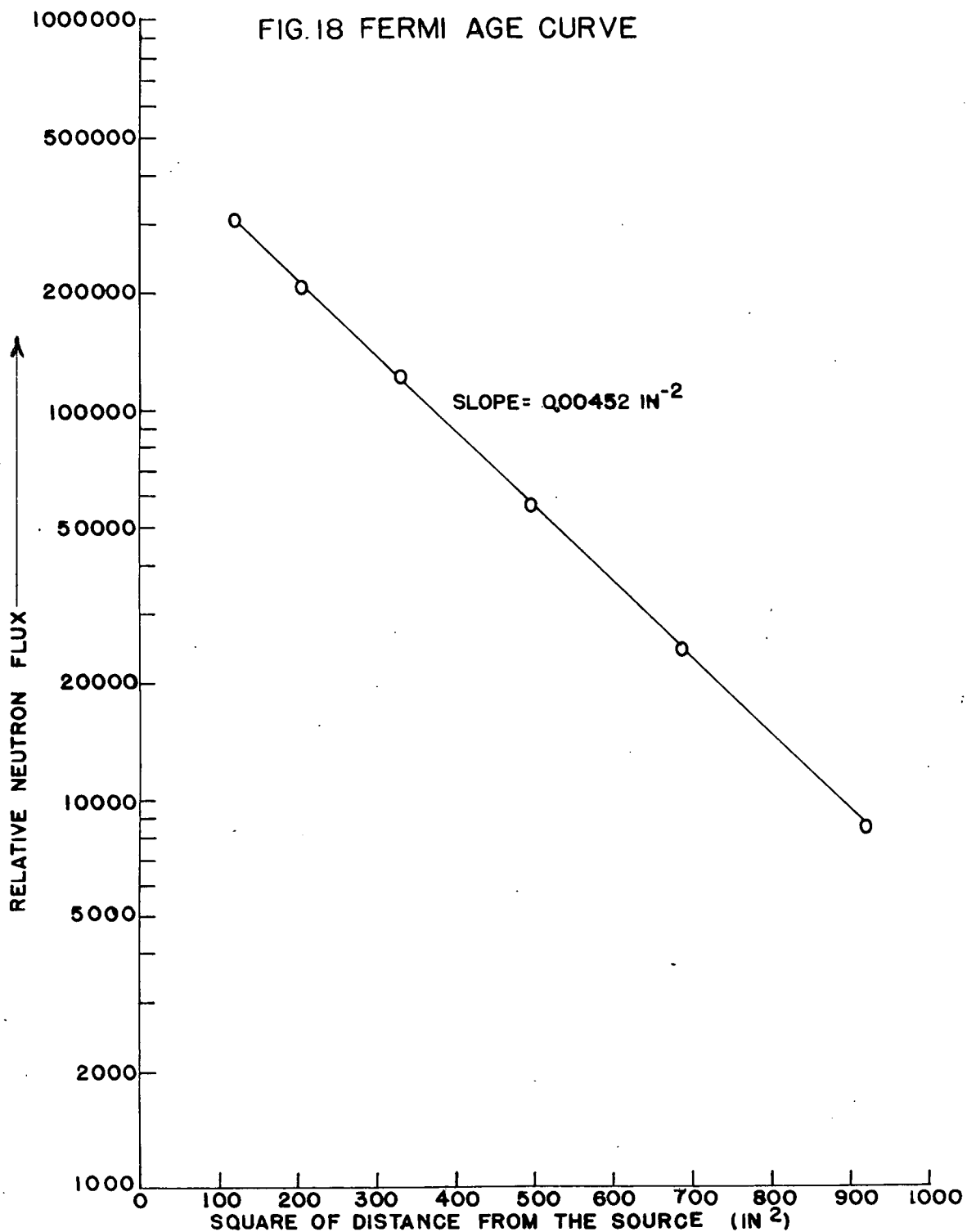
where:

$$\tau = \text{Fermi age.}$$

This gives a Fermi age of 357 cm^2 as compared to published value of 350 cm^2 for graphite⁽¹⁵⁾.

FIG. 17 DIFFUSION LENGTH CURVE





SUMMARY

A subcritical heterogeneous nuclear reactor was designed and constructed for use in the nuclear engineering program at Virginia Polytechnic Institute. Natural uranium fuel and reactor grade graphite were used as building materials.

Considering that no two samples of moderator have the same characteristics, the resulting parameters measured on this reactor are in good agreement with published data. The reactor performs the primary function as a versatile laboratory instrument that can measure as many reactor parameters as possible.

ACKNOWLEDGMENTS

The author wishes to express his appreciation to Dr. T. M. Hahn, Jr., for the guidance and inspiration so liberally given during the research and writing of this thesis. He would also like to thank Professor W. Richardson and the entire faculty of the Physics Department for the many helpful and time-saving suggestions given during the research period. The author is particularly indebted to Mr. L. Barnett for his long hours of assistance during the machining process.

Finally, the author wishes to extend special thanks to Mrs. E. P. Ellison for her care and interest in typing this thesis.

BIBLIOGRAPHY

1. Campbell, E. C., Wyly, L. D., Howell, E. I.,
AECD-3169, Measurements on the ORSORT
Uranium Graphite Exponential Pile, Atomic
Energy Commission, Oak Ridge, Tennessee,
1950.
2. Currie, L. M., Hamister, V. C., MacPherson, H. G.,
The Production and Properties of Graphite
for Reactors, National Carbon Co., 1955.
3. Downe, K. W., Kouts, H. J., Reactivity Coefficient
Measurements of Buckling, BNL-1785, Brook-
haven National Laboratory, Upton, New York.
4. Dopchie, H., Leonard, F., Neve de Meverguier, M.,
Touerneir, G., Conducting an Exponential
Experiment with a Natural-U Graphite Lattice,
Nucleonics, Vol. 14, No. 3, p. 57, March
1956.
5. Fermi, E., Experimental Production of a Divergent
Chain Reactor, American Journal of Physics,
Vol. 20, No. 9, p. 536, December 1952.
6. *ibid.*, p. 547.
7. Glasstone, S., Sourcebook on Atomic Energy, D. Van
Nostrand Co., New York, 1950.
8. Glasstone, S., Edlund, M. C., The Elements of
Nuclear Reactor Theory, D. Van Nostrand Co.,
New York, 1950.
9. *ibid.*, p. 84.
10. *ibid.*, p. 85.
11. *ibid.*, p. 53.
12. *ibid.*, p. 281.
13. *ibid.*, p. 285.

14. Glasstone, S., Edlund, M. C., The Elements of Nuclear Reactor Theory, D. Van Nostrand Co., New York, 1950, p. 208.
15. *ibid.*, p. 183.
16. Hughes, D. J., Pile Neutron Research, Addison-Wesley Publishing Co., Cambridge, Mass., 1953.
17. Jordon, E. D., The Design and Operation of a Subcritical Nuclear Reactor, New York University, 1955.
18. McCorkle, W. H., Using Intermediate Experiments for Reactor Nuclear Design, *Nucleonics*, Vol. 14, No. 3, p. 54, March 1956.
19. Murray, R. L., Introduction to Nuclear Engineering, Prentice-Hall, Inc., New York, 1954.
20. *ibid.*, p. 122.
21. *ibid.*, p. 116.
22. *ibid.*, p. 119.
23. *ibid.*, p. 334.
24. *ibid.*, p. 108.
25. Richey, C. R., Thermal Utilization and Lattice Diffusion Length in Graphite-Uranium Lattices from Exponential Pile Measurements, AECD-3675, Atomic Energy Commission, Oak Ridge, Tennessee.
26. Smith, A. B., An Experimental Study of Heterogeneous Exponential Assemblies, Argonne National Laboratory, 1955.

**The vita has been removed from
the scanned document**

APPENDIX I

CALCULATION OF RESONANCE ESCAPE PROBABILITY
AND THERMAL UTILIZATION FOR A CELL RADIUS
OF 8 CENTIMETERS

$$\underline{\text{Resonance Escape Probability}} = e^{-\frac{V_U \Sigma_U}{V_M \Sigma_M}}$$

$$\frac{S}{M} = \frac{R}{\rho_0 \rho} = .0842 \frac{\text{cm}^2}{\text{gm}}$$

$$V_U = 1.651 [1 + \mu \frac{S}{M}] = 1.651 + .371 = 2.022 \text{ BARN}$$

$$V_M = \frac{P}{5.6} = \frac{[.159][4.8]}{5.6} = .14 \text{ BARN}$$

$$V_U = \pi (1.27)^2 = 5.05 \text{ cm}^3$$

$$V_M = \pi (8)^2 = 5.05 \text{ cm}^3$$

$$\Sigma_M = \frac{P N_0}{A_M} V_M = [.0822][.14] = .0112 \text{ cm}^{-1}$$

$$\Sigma_U = \frac{P N_0}{A_U} V_U = [.0473][2.022] = .0955 \text{ cm}^{-1}$$

$$\text{Resonance Escape Probability} = e^{-\frac{(5.05 \times .0955)}{(5.05)(.0112)}} = .801$$

Thermal Utilization

$$\frac{1}{f} = 1 + \frac{V_M \Sigma_M}{V_U \Sigma_U} \cdot \frac{\phi(0)}{\phi} + \delta$$

$$\delta = \left(\frac{K_1 \eta_1}{2}\right)^2 \left(\ln \frac{\eta_1}{\eta_0} - \frac{3}{4}\right) = (2 \times 10^{-4})(64)(.99) = .0127$$

$$\frac{\phi(0)}{\phi} = 1 + \frac{(K_0 \eta_0)^2}{8} - \frac{(K_0 \eta_0)^4}{192} = 1 + \frac{.79}{8} - \frac{.625}{192} = 1.101$$

$$\frac{\Sigma_M}{\Sigma_U} = 1.07 \times 10^{-3}$$

$$\frac{V_M}{V_U} = 38.6$$

$$\frac{1}{f} = 1 + .0452 + .0127 = 1.057$$

$$f = \frac{1}{1.057} = .947$$

APPENDIX II

AN ANALYSIS OF THE FLUX DETERMINATION FOR THE FOIL AT
THE 10 INCH LEVEL WITH TWO LAYERS OF FUEL LOADED

Time of Irradiation = 1440 min.

Delay Time = 5 min.

Count Time = 1 min.

Total Counts/64 = 175.4.

Background Rate/64 = 1 counts/min.

Background Correction = 175.4 - 1 = 174.4 counts/64

$$\text{Error/64} = \pm \frac{.6745}{64(1 - e^{-0.128})} \sqrt{174.4 + \frac{(1)^2(1)^2}{58}} = \pm 86$$

$$\text{Relative Flux} = \frac{174.4}{(1 - e^{-0.128})} \pm 86 = 13,400 \pm 86$$

The calculations of the flux values for the four other loading measurements were divided by a factor of $e^{\lambda t}$ to normalize all loading data,

where:

λ = radioactive decay constant of polonium

t = time relative to first experiment.

The error factor was neglected when the data were plotted since there was less than 1 per cent error in each case.